PHYSICAL REVIEW B **85**, 014514 (2012)

Structural analysis and superconductivity of $CeFeAsO_{1-x}H_x$

Satoru Matsuishi,[1,*] Taku Hanna,[1] Yoshinori Muraba,[1] Sung Wng Kim,[2] Jung Eun Kim,[3] Masaki Takata,[3,4] Shin-ich Shamoto,[5] Ronald I. Smith,[6] and Hideo Hosono[1,2,†]

[1]*Materials and Structures Laboratory, Tokyo Institute of Technology, S2-13, 4259 Nagatsuta-cho, Midori-ku, Yokohama 226-8503, Japan*

[2]*Frontier Research Center, Tokyo Institute of Technology, 4259 Nagatsuta-cho, Midori-ku, Yokohama 226-8503, Japan*

[3]*Japan Synchrotron Radiation Research Institute, 1-1-1 Kouto, Sayo-cho, Sayo-gun, Hyogo 679-5198, Japan*

[4]*RIKEN SPring-8 Center, 1-1-1 Kouto, Sayo-cho, Sayo-gun, Hyogo 679-5148, Japan*

[5]*Quantum Beam Science Directorate, Japan Atomic Energy Agency, Tokai, Ibaraki 319-1195, Japan*

[6]*ISIS Facility, STFC Rutherford Appleton Laboratory, Harwell Oxford, Didcot, OX11 0QX, United Kingdom*

(Received 25 October 2011; published 19 January 2012)

We performed the neutron powder diffraction (NPD) and synchrotron x-ray diffraction measurements on $CeFeAsO_{1-x}(D,H)_x$ ($x = 0.0 - 0.48$) as a representative of 1111-type family of iron-based superconductors $LnFeAsO_{1-x}H_x$ (Ln = lanthanoid). Deuterated and hydrogenated samples ($CeFeAsO_{1-x}D_x$ and $CeFeAsO_{1-x}H_x$) were synthesized by the solid-state reaction of a metal oxide, arsenides, and a hydride and a deuteride source under an applied pressure of 2 GPa. No distinct differences were found between the structural and superconducting properties of the hydride and deuteride samples. Rietveld analyses of the NPD patterns demonstrated that deuterium exclusively substitutes on the oxygen sites in the 1111-type structures according to the nominal composition. Bulk superconductivity was observed over a wide x region ($0.1 < x < 0.4$) and the superconducting dome had a rather flat shape with a maximum $T_c = 47$ K at around $x = 0.25$. It was concluded from density functional theory calculations and comparison with the superconducting dome of the fluorine-substituted system that the charge state of the hydrogen substituting the oxygen sites was -1. The relationship between the lattice parameter a and T_c in our samples prepared from metal hydrides is almost the same as that reported previously for samples prepared from cerium hydroxide. These results strongly suggest that H^- ions exclusively occupy the oxygen sites in both samples, regardless of the hydrogen species in the starting material.

DOI: 10.1103/PhysRevB.85.014514 PACS number(s): 74.70.Xa, 74.62.Bf, 74.25.F−

I. INTRODUCTION

Since the discovery of the iron arsenide superconductors $LaFeAsO_{1-x}F_x$ ($T_c = 26$ K),[1] various types of parent materials have been reported, and their physical properties have been extensively studied.[2–9] Typical parent materials are 1111-type $LnFeAsO$ (Ln = lanthanoid)[1,10–13] and 122-type $AeFe_2As_2$ (Ae = alkaline-earth metal);[2,3,14] they show structural and antiferromagnetic transitions with stripe-type ordering in the iron square-lattice.[15–18] These transitions are suppressed by carrier doping via element substitution, and a superconductivity transition is induced instead. These results imply a scenario in which the superconductivity is intrinsically related to the magnetic interaction. The spin-fluctuation mechanism resulting from Fermi surface (FS) nesting between hole and electron pockets has been suggested as a plausible model.[19] This model explains well the suppression of superconductivity in 122-type $Ae(Fe_{1-x}Co_x)_2As_2$ upon electron doping to the level of filling up hole pockets[2,20,21] and several characteristic observations such as a striking difference between LaFeAsO and LaFePO. However, in contrast to the iron arsenides, the recently discovered alkali-metal-ion-intercalated iron selenide superconductor $K_xFe_{2-y}Se_2$,[9] also having an iron square lattice, shows different behavior; a high T_c of ∼30 K is retained even in a highly electron-doped state corresponding to the disappearance of hole pockets.[22,23] We therefore need to examine the validity of the FS nesting model as the major contributor to the superconductivity. Recently, we reported the synthesis of 1111-type $SmFeAsO_{1-x}H_x$ ($0 < x < 0.5$), using a high-pressure technique, and its superconductivity with a maximum T_c of 56 K at $x \sim 0.25$.[24] Although the hydrogen position in $SmFeAsO_{1-x}H_x$ could not be determined, this result suggests that the hydrogen forms a negative anion, i.e., H^-, at the oxygen site, releasing an electron to the FeAs layer ($O^{2-} \rightarrow H^- + e^-$), in the same way as fluorine does in $SmFeAsO_{1-x}F_x$.[10,11,25,26] By using the solubility limit of hydrogen ($x < 0.5$), which is much higher than that of fluorine ($x < 0.2$), we found that superconductivity is observed over a wide x region ($0.07 < x < 0.4$). According to density functional theory (DFT) calculations on the 1111-type system,[27] hole FS shrink at high electron-doping levels, i.e., $x >$ ∼0.3, but the observed T_c dome is insensitive to electron-doping levels of $x = 0.1 - 0.4$. These results imply that the FS nesting model is insufficient for explaining the superconductivity.

In this paper, use neutron powder diffraction (NPD) and synchrotron x-ray diffraction (SXRD), with the aid of density functional theory (DFT) calculations, to we demonstrate that hydrogen exclusively occupies the oxygen sites and donates an electron to the FeAs layer in $CeFeAsO_{1-x}(H,D)_x$, representing $LnFeAsO_{1-x}H_x$. $CeFeAsO_{1-x}(H,D)_x$ systems show a wide superconducting dome ($0.1 < x < 0.4$) with a maximum T_c of 47 K at $x = 0.25$. The present results are compared with those for OH-doped samples.[28]

II. EXPERIMENTAL

$CeFeAsO_{1-x}D_x$ was synthesized by the solid-state reaction of CeAs, Fe_2As, CeO_2, and CeD_2 ($CeAs + Fe_2As + (1-x)\,CeO_2 + x\,CeD_2 \rightarrow 2CeFeAsO_{1-x}D_x$), using a belt-type high-pressure anvil cell. CeAs and Fe_2As were prepared from

their respective metals, and CeD_2 was synthesized by heating cerium metal in a D_2 atmosphere. All starting materials and precursors for the synthesis were prepared in a glove box filled with purified Ar gas (H_2O, O_2 <1 ppm). The mixture of starting materials was placed in a BN capsule with a mixture of $Ca(OD)_2$ and $NaBD_4$ as an excess deuterium source and then heated at 1473 K and 2 GPa for 30 min. The hydride analog, $CeFeAsO_{1-x}H_x$, was prepared in an identical fashion, but using CeH_2, $Ca(OH)_2$, and $NaBH_4$.[29]

To determine the framework structure (site positions and occupancies of Ce, Fe, and As), SXRD data were collected at 300 K from $CeFeAsO_{1-x}H_x$ (nominal $x = 0.0$, 0.1, 0.3, 0.4, and 0.5) using the BL02B2 beamline at SPring-8, Japan The x-ray wavelength was set at 0.049920 nm. Rietveld analyses of the SXRD patterns were performed using the RIETAN-FP code.[30] In order to determine the deuterium (hydrogen) distribution in these compounds, time-of-flight (TOF) NPD data collected from $CeFeAsO_{1-x}D_x$ (nominal $x = 0.0$, 0.1, 0.3, and 0.4) were measured using GEM diffractometer at the ISIS pulsed spallation neutron source, Rutherford Appleton Laboratry, UK.[31] Rietveld analyses of the TOF-NPD patterns were carried out using the General Structure Analysis System (GSAS) code.[32]

The amounts of hydrogen incorporated in the resulting samples were evaluated by thermogravimetry and mass spectroscopy (TG-MS) performed using a TG-MS (Bruker AXS GmbH model TG-DTA/MS 9610) equipped with a gas feed port to inject the standard H_2 gas into the sample chamber.[24] Approximately 20 mg of sample were heated to 1073 K at a heating rate of 20 K/min under a helium gas flow. Hydrogen released from the sample, in the form of H_2 molecules, was ionized and detected by a quadrupole mass spectrometer as an ion with a mass-to-charge ratio $(m/z) = 2$. Elemental compositions, except hydrogen (Ce:Fe:As:O), were determined using an electron-probe microanalyzer (EPMA, JEOL, Inc. model JXA-8530F) equipped with a field-emission-type electron gun and wavelength dispersive x-ray detectors. The micrometer scale compositions within the main phase were probed on five to ten focal points, and the results were averaged.

Four-probe dc resistivity (ρ) and magnetic susceptibility (χ) were measured in the temperature range of 2−300 K using a physical properties measurement system (Quantum Design, Inc.) with a vibrating sample magnetometer attachment.

TABLE I. Analyzed elemental compositions of $CeFeAsO_{1-x}H_x$.

$x_{nominal}$	[Ce]	[Fe]	[As]	[O]	[H]
0.03	1.01	1	0.99	0.95	0.03
0.07	1.01	1	1.00	0.89	0.07
0.10	1.00	1	1.00	0.86	0.10
0.20	1.00	1	1.00	0.74	0.22
0.30	1.01	1	0.99	0.73	0.32
0.40	1.01	1	1.01	0.60	0.40
0.50	1.00	1	1.00	0.53	0.48

DFT calculations were performed using the generalized gradient approximation Perdew-Burke-Ernzerhof functional,[33,34] and the projected augmented plane-wave method[35] implemented in the Vienna *ab initio* simulation program code.[36] A $\sqrt{2}a \times \sqrt{2}a \times 2c$ supercell containing eight chemical formulas was used, and the plane-wave basis-set cutoff was set to 600 eV. Referring to the previous theoretical work by Liu *et al.*,[37] the value of the effective on-site Coulomb interaction U_{eff} $(=U-J)$ was fixed to be 0.0 eV for Fe and 3.0 eV for Ce, where U is the on-site Coulomb repulsion and J is the exchange coupling. For Brillouin-zone integrations to calculate the total energy and density of states (DOS), $8 \times 8 \times 4$ Monkhorst-Pack grids of k points were used. To obtain the projected DOS (PDOS), the charge density was decomposed over the atom-centered spherical harmonics with a Wigner-Seitz radius $r = (3V_{cell}/4\pi N)^{1/3}$, where V_{cell} and N are the unit-cell volume and the number of atoms in a unit cell, respectively.

III. RESULTS AND DISCUSSION

$CeFeAsO_{1-x}D_x$ and $CeFeAsO_{1-x}H_x$ were synthesized for nominal x values ($x_{nominal}$) of 0.0−0.5. A few percent of CeAs and unknown impurity phases segregated for $x_{nominal} =$ 0.0 and $x_{nominal} \geqslant 0.4$, but a single phase was obtained for $x_{nominal} = 0.1 - 0.3$. Table I summarizes the elemental compositions ([Ce]:[Fe]:[As]:[O]:[H]), normalized by the molar content of iron, determined for each sample using EPMA

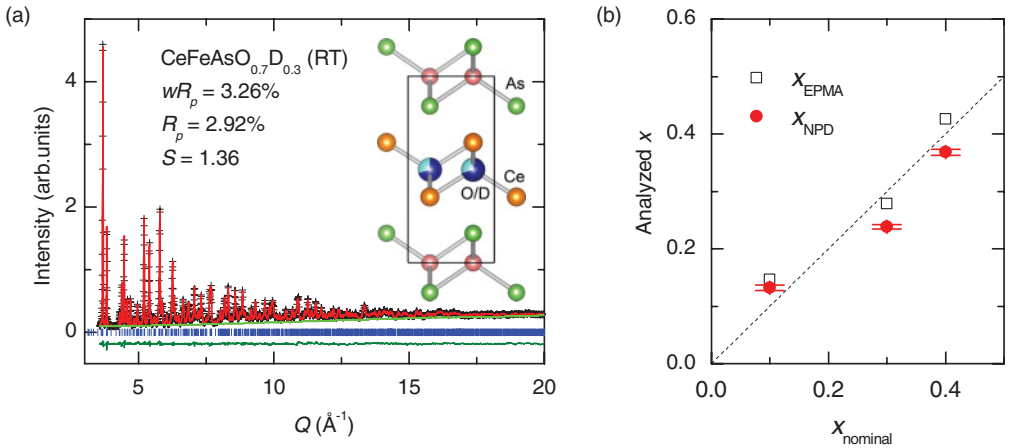

FIG. 1. (Color online) (a) Fitted NPD pattern of $CeFeAsO_{0.7}D_{0.3}$ at RT and (b) deuterium contents obtained by Rietveld analyses of NPD patterns and oxygen content obtained by EPMA as a function of nominal composition x.

TABLE II. Refined structural parameters of $CeFeAsO_{1-x}D_x$ at 300 K.

Space group: $P4/nmm$ (Origin choice 2), Ce: $2c$ (1/4, 1/4, z_{Ce}) Fe: $2a$ (3/4, 1/4, 0) As: $2c$ (1/4, 1/4, z_{As}) O/D: $2b$ (3/4, 1/4, 1/2)

$x_{nominal}$	[O]	g_D	a (Å)	c (Å)	z_{Ce}	z_{As}	wRp (%)	Rp (%)	S
0	1.0	0	4.00033(3)	8.65926(10)	0.63990(16)	0.15476(12)	3.94	3.21	1.57
0.1	0.854	0.132(5)	3.99812(4)	8.63525(12)	0.64124(16)	0.15589(12)	3.29	2.70	1.38
0.3	0.721	0.238(4)	3.97749(3)	8.60913(11)	0.64639(16)	0.15869(13)	3.26	2.92	1.36
0.4	0.574	0.368(5)	3.95386(4)	8.59259(12)	0.65145(20)	0.16340(16)	3.93	3.30	1.48

and TG-MS. Figure 1(a) shows TOF-NPD patterns ($\langle 2\theta \rangle = 154.46^\circ$ detector bank) of $CeFeAsO_{0.7}D_{0.3}$ at room temperature (RT) along with the fitted pattern. All the peaks could be indexed to a tetragonal ZrCuSiAs-type structure (space group: $P4/nmm$),[38] with the lattice parameters $a = 0.3978$ nm and $c = 0.8609$ nm for $CeFeAsO_{0.7}D_{0.3}$. Rietveld analysis was performed with a structural model in which deuterium replaces a fraction of oxygen sites in the 1111-type structure. The values of the temperature factors (U_{iso}) for Ce, Fe, As, and O were fixed at those in a undoped sample, and U_{iso} of D was fixed at that of oxygen. Good agreement was obtained between the calculated and observed patterns (reliability factor $wR_p = 3.26\%$ and goodness of fit $S = 1.36$) when the site occupancy of deuterium (g_D) corresponding to x was equal to 0.24. Because the coherent neutron scattering length of deuterium (6.671 fm) is similar to that of oxygen (5.803 fm),[39] the result of the pattern fitting for $CeFeAsO_{0.7}D_{0.3}$ indicates that at least 96% of the oxygen sites in the CeO layer are occupied by deuterium or oxygen. Taking into account the isotopic purity of the CeD_2 and external deuteron source, $Ca(OD)_2$ and $NaBD_4$, and the inclusion of hydrogen from other starting materials, we consider that the remaining fraction (0.04) of the oxygen sites is primarily occupied by hydrogen. Figure 1(b) compares the x values in $CeFeAsO_{1-x}D_x$ obtained by NPD (x_{NPD}) and the oxygen concentration measured by EPMA (x_{EPMA}) as a function of nominal x in the starting materials. Both values agree well with the nominal x in all samples. The underestimation of x_{NPD} may be accounted for by the hydrogen incorporation described above. We also examined the validities of other structural models, with interlayer hydrogen[40] and oxygen vacancies.[41–43] However, these models yield quite large wR_p values (>10%), indicating that these structural models are inappropriate.

Table II lists the structural parameters of deuterated samples at RT. All the refinements yield good fits between

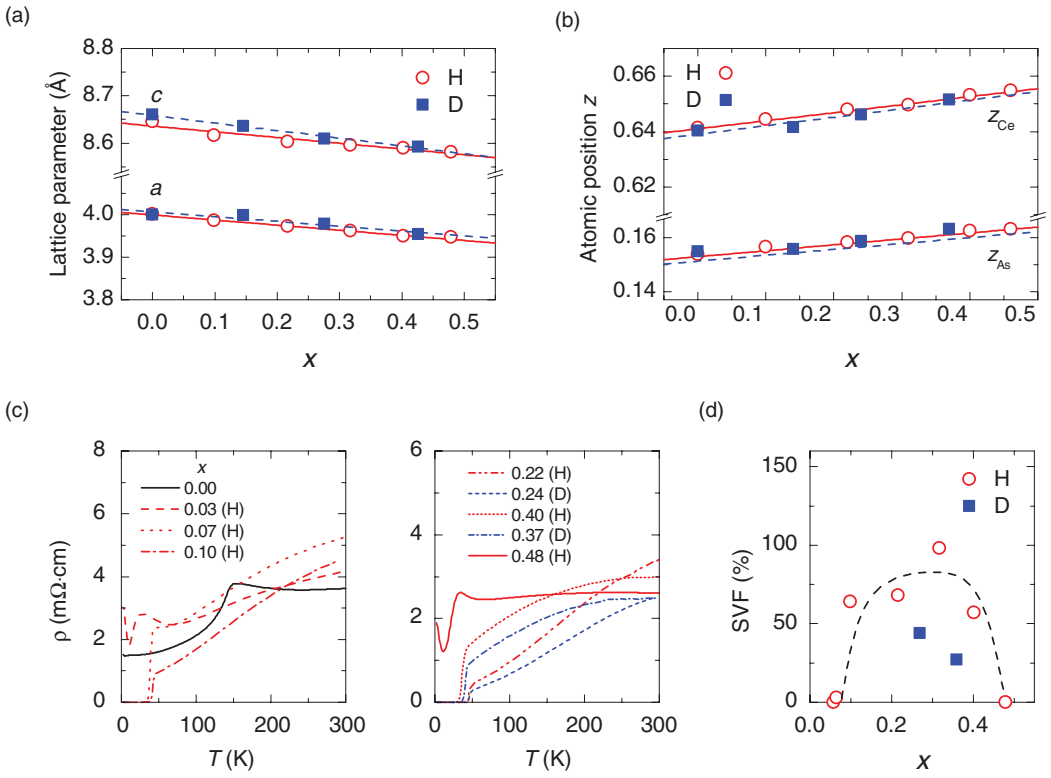

FIG. 2. (Color online) Structural and superconductivity data. (a) Variations in lattice parameters (a and c) as a function of x; (b) atomic positions z (z_{Ce} and z_{As}) of $CeFeAsO_{1-x}H_x$ and $CeFeAsO_{1-x}D_x$ measured by SXRD and NPD; (c) ρ–T profile of $CeFeAsO_{1-x}H_x$ (solid line) and $CeFeAsO_{1-x}D_x$ (open circles) in underdoped (left, $x = 0.00 - 0.10$) and overdoped states (right, $x = 0.22 - 0.48$) systems; and (d) shielding volume fractions of $CeFeASO_{1-x}H_x$ and $CeFeAsO_{1-x}D_x$ estimated from M–H curve at 2 K and 10 Oe.

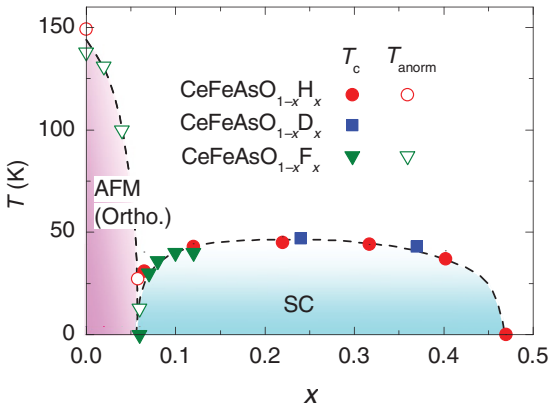

FIG. 3. (Color online) x–T diagrams of $CeFeAsO_{1-x}H_x$ and $CeFeAsO_{1-x}D_x$ superimposed by data reported for $CeFeAsO_{1-x}F_x$ (Ref. 18).

observed and calculated profiles, with reliability factors of $S < 1.57$, $wR_p < 3.94\%$, and $R < 3.30\%$. Figures 2(a) and 2(b) show the variations in the lattice parameters (a and c) and the atomic positions of arsenic and cerium in the deuterated and hydrated samples, obtained by SXRD and NPD analyses as a function of x, respectively. The lengths of the $a-$ and $c-$axes monotonically decreased with increasing x up to 0.48, and no significant differences in the lattice parameters or atomic positions were noted between the hydrogenated and deuterated samples. These results indicate that the solubility limit of the hydrogen species is extended up to 48% and that there is no significant isotopic effect on the crystal structure. Furthermore, the consistency of the XRD and NPD results substantiates the suggestion that the hydrogen exclusively substitutes the oxygen sites (see supplemental material[44]).

Figure 2(c) shows the temperature dependence of the resistivity in deuterated and hydrogenated samples. A sudden drop in resistivity as a result of superconductivity is observed from $x = 0.1$ to 0.4. Figure 2(d) shows the shielding volume fraction (SVF) evaluated from the slope of the magnetization vs magnetic field (M–H) curve. An SVF larger than 20% was obtained for a wide doping range. No significant isotopic effect was observed for the resistivity and T_c.

Figure 3 shows the phase diagrams of $CeFeAsO_{1-x}H_x$ and $CeFeAsO_{1-x}D_x$ along with that of the fluorine-substituted system $CeFeAsO_{1-x}F_x$.[18] Here, T_c is the onset superconducting transition temperature obtained from the χ–T curve, and T_{anom} denotes a breaking point in the ρ–T curve. A wide T_c dome ranging from $x = 0.1$ to 0.4 and the disappearance of superconductivity at $x > 0.4$ were observed for the hydrogen-substituted 1111 system; these were not observed in the fluorine-substituted system because of small solubility of fluorine ($x < 0.2$). The maximum T_c, 47 K, is higher than that (41 K) in the fluorine-substituted system.[12] According to our results on CaFeAsH,[24] the hydrogens in the oxygen sites exist as H^- ions.

To investigate the effects of hydrogen substitution, we performed DFT calculations on CeFeAsO, $CeFeAsO_{0.75}F_{0.25}$, and $CeFeAsO_{0.75}H_{0.25}$ systems. Figure 4(a) shows the supercell used for the DFT calculations; it contains eight anion sites in the blocking layer. For $CeFeAsO_{0.75}F_{0.25}$ and $CeFeAsO_{0.75}H_{0.25}$, 1/4 of the oxygen sites were replaced by fluorine or hydrogen. The lattice parameters and atomic positions were fully relaxed by a structural optimization procedure minimizing the total energy and force (see supplemental material[45]). Although a noncollinear spin configuration was suggested for CeFeAsO by previous NPD and DFT studies,[18,37] a collinear configuration was assumed in our calculation to decrease the calculation costs. As a result of energy optimization, an orthorhombic antiferromagnetic ground state was obtained for CeFeAsO, with stripe-type ordering in the Fe lattice and checkerboard-type ordering in the Ce lattice [see Fig. 4(a)]. The values of the local moments for Fe and Ce (1.9 and 0.9 μ_B) agree well with those calculated in a previous theoretical study.[37] Contrary to the experimental results, magnetic ordering still remained in $CeFeAsO_{0.75}F_{0.25}$ and $CeFeAsO_{0.75}H_{0.25}$; this reveals the limitations of DFT, which is inadequate for reproducing low-energy phenomena

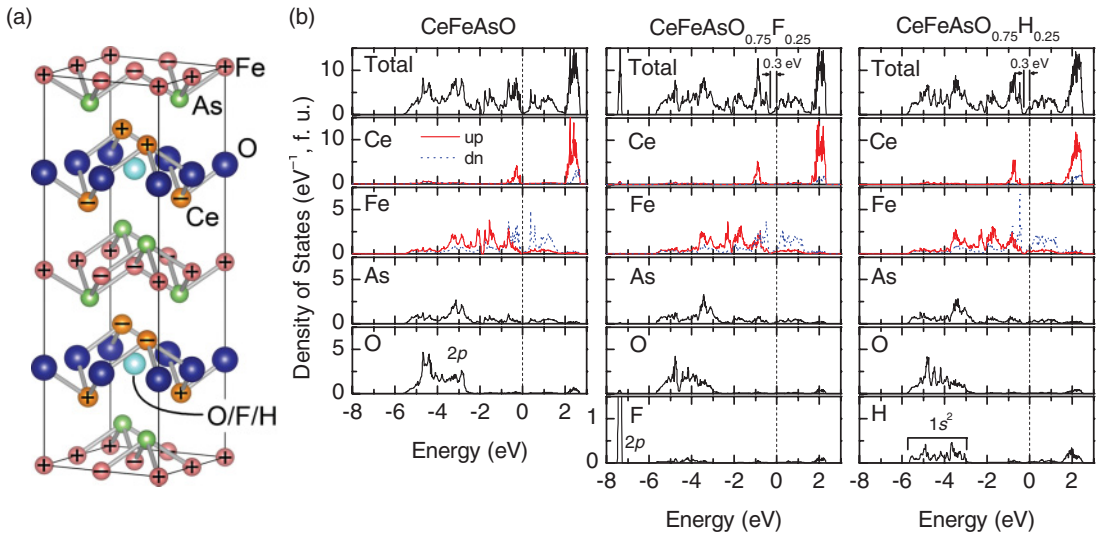

FIG. 4. (Color online) Electronic structures: (a) structural model for DFT calculations; "+" and "−" on the Ce and Fe atoms indicate the signs of the spin magnetic moment. (b) Total DOS and atomic PDOS of CeFeAsO, $CeFeAsO_{0.75}F_{0.25}$, and $CeFeAsO_{0.75}H_{0.25}$, obtained by DFT calculations. The origin was set at the Fermi level.

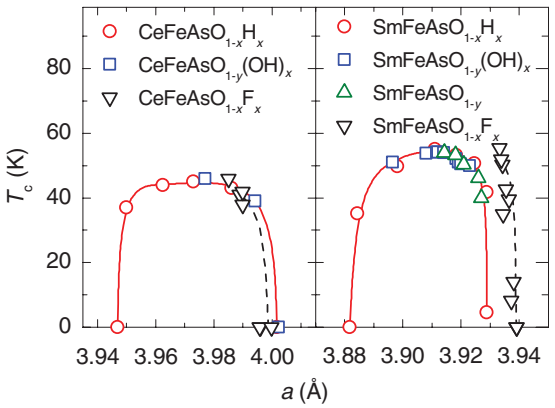

FIG. 5. (Color online) Critical temperatures of $LnFeAsO_{1-x}H_x$ (Ln = Ce and Sm) as a function of lattice parameters a, superimposed by those of $LnFeAsO_{1-y}(OH)_x$ $LnFeAsO_{1-y}$, and $LnFeAsO_{1-x}F_x$. (Refs. 12, 18, 28, 43, 46–51.)

in the Fe-arsenide system. However, this calculation result is still effective for discussing the bonding states. Figure 4(b) compares the total and projected DOS per formula unit (f.u.) for CeFeAsO, $CeFeAsO_{0.75}F_{0.25}$, and $CeFeAsO_{0.75}H_{0.25}$. In $CeFeAsO_{0.75}F_{0.25}$, the fluorine forms a narrow isolated $2p$ band located at -8 eV from the Fermi level (E_f). In contrast, the hydrogen in $CeFeAsO_{0.75}H_{0.25}$ forms a broad $1s$ band located at -3 to -6 eV, which is close to that of the oxygen $2p$ band, demonstrating that the hydrogen $1s$ and oxygen $2p$ orbitals energetically overlap and form a unified valence band. The integrated PDOS for the hydrogen 1s band is 0.5 electrons per f.u., corresponding to the H^- state ($1s^2$). Furthermore, both fluorine and hydrogen substitutions push up the E_F by 0.3 eV, corresponding to a doping of 0.25 electrons per Fe. We therefore now conclude that the hydrogen substituting the oxygen site forms a negative anion, i.e., H^-, donating an electron to the FeAs layer, the same as F^- does. This is consistent with a close overlap of the T_c domes of hydrogen-substituted and fluorine-substituted systems.

Here, we would like to point out a close similarity between the phase diagrams of our hydride-doped samples $LnFeAsO_{1-x}(H,D)_x$, where Ln = Ce and Sm, and those of the hydroxyl-doped samples $LnFeAsO_{1-y}(OH)_x$ reported in Ref. 46. The OH-doped samples were prepared using the hydroxides $Sm(OH)_3$ and $Ce(OH)_3$ as starting materials. Unfortunately, neither the chemical states nor the crystallographic positions have been reported, as far as we know. Figure 5 shows the relation between T_c and the a-axis dimension for both series of samples. It is evident that all the data for both series fall on a common curve for the Sm and Ce systems. This agreement suggests that hydrogen species occupy the oxygen sites of $LnFeAsO_{1-x}H_x$ as H^- ions, regardless of the starting materials. Finally, we compare the present a-T_c curve with that for $LnFeAsO_{1-x}F_x$ synthesized at an ambient-pressure (see Fig. 5).[12,18,47–51] Depending on the pressure condition of synthesis, the value of a is significantly different even for nonsubstituted samples.[52] However, the line shape of a-T_c curve for $LnFeAsO_{1-x}F_x$ is similar to that of $LnFeAsO_{1-x}H_x$. This result implies extent of band filling is a primary factor for T_c. Because the ionic radius of H^- is similar to that of O^{2-} and the solubility limit of H^- in the 1111 system is rather larger than F^-, the use of H^- ions would be an effective electron-doping method.

IV. SUMMARY

We succeeded in synthesizing $CeFeAsO_{1-x}H_x$ and $CeFeAsO_{1-x}D_x$ in the range up to $x = 0.48$ under a pressure of 2 GPa. Diffraction studies revealed that hydrogen species exclusively substitute the oxygen sites in the CeO layer, and DFT calculations indicated that the charge state of the hydrogen or deuterium is -1. No isotopic effect was noted in the structural and superconducting properties of the substituted samples. The x–T phase diagram shows a wide superconducting region ($0.1 < x < 0.4$) with a maximum T_c of 47 K at $x = 0.25$. The value of T_c remained almost constant in the range $0.1 < x < 0.4$, and this feature was similar to that for $SmFeAsO_{1-x}H_x$, except for the maximum T_c value. Although the solubility limit ($x \sim 0.48$) of H^- is rather different from that (0.12) of F^-, the phase diagram of $CeFeAsO_{1-x}H_x$ agreed with that of $CeFeAsO_{1-x}F_x$ in the range $x < 0.12$. This result substantiates the idea that hydrogen occurs as negative anions, i.e., H^-, supplying electrons to the FeAs layer, the same as fluorine does. It turned out from these results that T_c of the 1111-type system is insensitive to electron doping. The close agreement in the relation between T_c and the unit cell axes dimensions among the samples prepared from LnH_2 and $Ln(OH)_3$ strongly suggests that the hydrogens in 1111 iron arsenide exclusively occupy the oxygen sites as H^- ions, irrespective of the hydrogen species (H^- or OH^-) in the starting materials.

ACKNOWLEDGMENT

This research is funded by the Japan Society for the Promotion of Science (JSPS) through the FIRST program, initiated by the Council for Science and Technology Policy (CSTP). GEM Xpress Access neutron beamtime was provided by the UK Science and Technology Facilities Council (STFC). The synchrotron radiation experiments were performed at the BL02B2 of SPring-8 with the approval of the Japan Synchrotron Radiation Research Institute (JASRI) (proposal NO. 2011A1142).

*satoru@lucid.msl.titech.ac.jp
†hosono@msl.titech.ac.jp

[1] Y. Kamihara, T. Watanabe, M. Hirano, and H. Hosono, J. Am. Chem. Soc. **130**, 3296 (2008).
[2] M. Rotter, M. Tegel, and D. Johrendt, Phys. Rev. Lett. **101**, 107006 (2008).
[3] C. Gen-Fu, L. Zheng, L. Gang, H. Wan-Zheng, D. Jing, Z. Jun, Z. Xiao-Dong, Z. Ping, W. Nan-Lin, and L. Jian-Lin, Chin. Phys. Lett. **25**, 3403 (2008).
[4] G. Wu, H. Chen, T. Wu, Y. L. Xie, Y. J. Yan, R. H. Liu, X. F. Wang, J. J. Ying, and X. H. Chen, J. Phys. Condens. Matter **20**, 422201 (2008).

[5]F.-C. Hsu, J.-Y. Luo, K.-W. Yeh, T.-K. Chen, T.-W. Huang, P. M. Wu, Y.-C. Lee, Y.-L. Huang, Y.-Y. Chu, D.-C. Yan, and M.-K. Wu, Proc. Natl. Acad. Sci. USA **105**, 14262 (2008).
[6]H. Ogino, Y. Matsumura, Y. Katsura, K. Ushiyama, S. Horii, K. Kishio, and J. Shimoyama, Supercon. Sci. Technol. **22**, 075008 (2009).
[7]X. Zhu, F. Han, G. Mu, P. Cheng, B. Shen, B. Zeng, and H.-H. Wen, Phys. Rev. B **79**, 220512(R) (2009).
[8]G. F. Chen, T.-L. Xia, H. X. Yang, J. Q. Li, P. Zheng, J. L. Luo, and N. L. Wang, Supercon. Sci. Technol. **22**, 072001 (2009).
[9]J. Guo, S. Jin, G. Wang, S. Wang, K. Zhu, T. Zhou, M. He, and X. Chen, Phys. Rev. B **82**, 180520 (2010).
[10]X. H. Chen, T. Wu, G. Wu, R. H. Liu, H. Chen, and D. F. Fang, Nature **453**, 761 (2008).
[11]A. Ren, W. Lu, J. Yang, W. Yi, X.-L. Shen, Z.-C. Li, G.-C. Che, X.-L. Dong, L.-L. Sun, F. Zhou, and Z-X. Zhao, Chin. Phys. Lett. **25**, 2215 (2008).
[12]G. F. Chen, Z. Li, D. Wu, G. Li, W. Z. Hu, J. Dong, P. Zheng, J. L. Luo, and N. L. Wang, Phys. Rev. Lett. **100**, 247002 (2008).
[13]Z.-A. Ren, J. Yang, W. Lu, W. Yi, X.-L. Shen, Z.-C. Li, G.-C. Che, X.-L. Dong, L.-L. Sun, F. Zhou, and Z.-X. Zhao, Europhys. Lett. **82**, 57002 (2008).
[14]K. Sasmal, B. Lv, B. Lorenz, A. M. Guloy, F. Chen, Y.-Y. Xue, and C.-W. Chu, Phys. Rev. Lett. **101**, 107007 (2008).
[15]Q. Huang, Y. Qiu, W. Bao, M. A. Green, J. W. Lynn, Y. C. Gasparovic, T. Wu, G. Wu, and X. H. Chen, Phys. Rev. Lett. **101**, 257003 (2008).
[16]C. H. Lee, K. Kihou, H. Kawano-Furukawa, T. Saito, A. Iyo, H. Eisaki, H. Fukazawa, Y. Kohori, K. Suzuki, H. Usui, K. Kuroki, and K. Yamada, Phys. Rev. Lett. **106**, 067003 (2011).
[17]C. de la Cruz, Q. Huang, J. W. Lynn, J. Li, W. R. II, J. L. Zarestky, H. A. Mook, G. F. Chen, J. L. Luo, N. L. Wang, and P. Dai, Nature **453**, 899 (2008).
[18]J. Zhao, Q. Huang, C. de la Cruz, S. Li, J. W. Lynn, Y. Chen, M. A. Green, G. F. Chen, G. Li, Z. Li, J. L. Luo, N. L. Wang, and P. Dai, Nat. Mater. **7**, 953 (2008).
[19]I. I. Mazin, D. J. Singh, M. D. Johannes, and M. H. Du, Phys. Rev. Lett. **101**, 057003 (2008).
[20]M. Rotter, M. Pangerl, M. Tegel, and D. Johrendt, Angew. Chem. Int. Ed. Engl. **47**, 7949 (2008).
[21]Y. Sekiba, T. Sato, K. Nakayama, K. Terashima, P. Richard, J. H. Bowen, H. Ding, Y.-M. Xu, L. J. Li, G. H. Cao, Z.-A. Xu, and T. Takahashi, New J. Phys. **11**, 025020 (2009).
[22]Y. Zhang, L. X. Yang, M. Xu, Z. R. Ye, F. Chen, C. He, H. C. Xu, J. Jiang, B. P. Xie, J. J. Ying, X. F. Wang, X. H. Chen, J. P. Hu, M. Matsunami, S. Kimura, and D. L. Feng, Nat. Mater. **10**, 273 (2011).
[23]T. Sato, K. Nakayama, Y. Sekiba, P. Richard, Y. M. Xu, S. Souma, T. Takahashi, G. F. Chen, J. L. Luo, N. L. Wang, and H. Ding, Phys. Rev. Lett. **103**, 047002 (2009).
[24]T. Hanna, Y. Muraba, S. Matsuishi, N. Igawa, K. Kodama, S. I. Shamoto, and H. Hosono, Phys. Rev. B **84**, 024521 (2011).
[25]A. Köhler and G. Behr, J. Supercond. Nov. Magn. **22**, 565 (2009).
[26]T. Tohei, T. Mizoguchi, H. Hiramatsu, Y. Kamihara, H. Hosono, and Y. Ikuhara, Appl. Phys. Lett. **95**, 193107 (2009).
[27]K. Kuroki, H. Usui, S. Onari, R. Arita, and H. Aoki, Phys. Rev. B **79**, 224511 (2009).
[28]K. Miyazawa, S. Ishida, K. Kihou, P. M. Shirage, M. Nakajima, C. H. Lee, H. Kito, Y. Tomioka, T. Ito, H. Eisaki, H. Yamashita, H. Mukuda, K. Tokiwa, S. Uchida, and A. Iyo, Appl. Phys. Lett. **96**, 072514 (2010).
[29]M. Iwamoto and Y. Fukai, Mater. Trans. JIM **40**, 606 (1999).
[30]F. Izumi and K. Momma, Solid State Phenom. **130**, 15 (2007).
[31]A. C. Alex, Nucl. Instrum. Methods **551**, 88 (2005).
[32]A. C. Larson and R. B. Von Dreele, *General Structure Analysis System (GSAS) Los Alamos National Laboratory Report LAUR 86-748* (Los Alamos National Laboratory, Los Alamos, New Mexico, 2004).
[33]J. P. Perdew, K. Burke, and M. Ernzerhof, Phys. Rev. Lett. **77**, 3865 (1996).
[34]J. P. Perdew, K. Burke, and M. Ernzerhof, Phys. Rev. Lett. **78**, 1396 (1997).
[35]P. E. Blöchl, Phys. Rev. B **50**, 17953 (1994).
[36]G. Kresse and J. Furthmüller, Phys. Rev. B **54**, 11169 (1996).
[37]J. Liu, B. Luo, Z. Y. Sun, H. Fu, and K. Yao, Phys. Rev. B **84**, 115123 (2011).
[38]R. Pottgen and D. Johrendt, Z. Naturforsch. **63b**, 1135 (2008).
[39]V. F. Sears, Neutron News **3**, 26 (1992).
[40]H. Nakamura and M. Machida, Physica C **471**, 662 (2011).
[41]Z.-A. Ren, G.-C. Che, X.-L. Dong, J. Yang, W. Lu, W. Yi, X.-L. Shen, Z.-C. Li, L.-L. Sun, F. Zhou, and Z.-X. Zhao, Europhys. Lett. **83**, 17002 (2008).
[42]H. Kito, H. Eisaki, and A. Iyo, J. Phys. Soc. Jpn. **77**, 063707 (2008).
[43]K. Miyazawa, K. Kihou, P. M. Shirage, C.-H. Lee, H. Kito, H. Eisaki, and A. Iyo, J. Phys. Soc. Jpn. **78**, 034712 (2009).
[44]See Supplemental Material at http://link.aps.org/supplemental/10.1103/PhysRevB.85.014514 for crystallographic information files (CIF) files containing crystallographic information of $CeFeAsO_{1-x}(H,D)_x$ crystals obtained by Rietveld refinements of XRD and NPD patterns.
[45]See Supplemental Material at http://link.aps.org/supplemental/10.1103/PhysRevB.85.014514 for DFT-optimized crystal structures.
[46]P. M. Shirage, K. Miyazawa, K. Kihou, H. Kito, Y. Yoshida, Y. Tanaka, H. Eisaki, and A. Iyo, Phys. Rev. Lett. **105**, 037004 (2010).
[47]Y. Kamihara, T. Nomura, M. Hirano, J. Eun Kim, K. Kato, M. Takata, Y. Kobayashi, S. Kitao, S. Higashitaniguchi, Y. Yoda, M. Seto, and H. Hosono, New J. Phys. **12**, 033005 (2010).
[48]A. Martinelli, M. Ferretti, P. Manfrinetti, A. Palenzona, M. Tropeano, M. R. Cimberle, C. Ferdeghini, R. Valle, C. Bernini, M. Putti, and A. S. Siri, Supercon. Sci. and Technol. **21**, 095017 (2008).
[49]N. D. Zhigadlo, S. Katrych, Z. Bukowski, S. Weyeneth, R. Puzniak, and J. Karpinski, J. Phys. Condens. Matter **20**, 342202 (2008)
[50]L. Sun, X. Dai, C. Zhang, W. Yi, G. Chen, N. Wang, L. Zheng, Z. Jiang, X. Wei, Y. Huang, J. Yang, Z. Ren, W. Lu, X. Dong, G. Che, Q. Wu, H. Ding, J. Liu, T. Hu, and Z. Zhao, Europhys. Lett. **91**, 57008 (2010).
[51]F. Bondino, E. Magnano, C. H. Booth, F. Offi, G. Panaccione, M. Malvestuto, G. Paolicelli, L. Simonelli, F. Parmigiani, M. A. McGuire, A. S. Sefat, B. C. Sales, R. Jin, P. Vilmercati, D. Mandrus, D. J. Singh, and N. Mannella, Phys. Rev. B **82**, 014529 (2010).
[52]K. Kodama, M. Ishikado, F. Esaka, A. Iyo, H. Eisaki, and Shin-ichi Shamoto, J. Phys. Soc. Jpn. **80**, 034601 (2011).